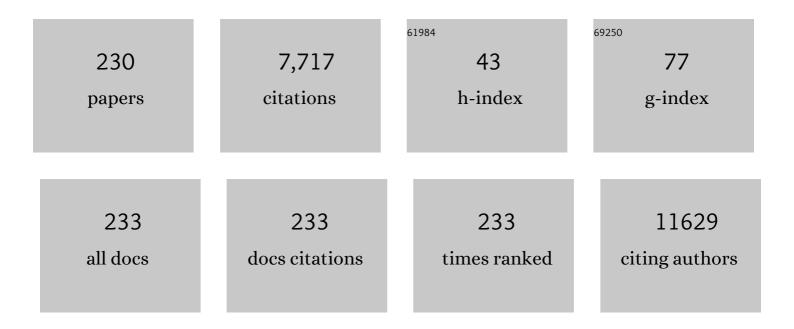
## Chao Liu

List of Publications by Year in descending order

Source: https://exaly.com/author-pdf/212357/publications.pdf Version: 2024-02-01



Силотии

#	Article	IF	CITATIONS
1	Modified Arytenoid Adduction Operation for the Treatment of Unilateral Vocal Fold Paralysis. Orl, 2022, 84, 205-210.	1.1	2
2	The Stochastic Augmented Lagrangian method for domain adaptation. Knowledge-Based Systems, 2022, 235, 107593.	7.1	3
3	Mortality salience enhances neural activities related to guilt and shame when recalling the past. Cerebral Cortex, 2022, 32, 5145-5162.	2.9	3
4	Effects of transcranial direct current stimulation over the right dorsolateral prefrontal cortex on fairness-related decision-making. Social Cognitive and Affective Neuroscience, 2022, 17, 695-702.	3.0	6
5	Self-Assembly of Chiral Ferrocene-Functionalized Polyoxotitanium Clusters for Photocatalytic Selective Sulfide Oxidation. Inorganic Chemistry, 2022, 61, 2903-2910.	4.0	3
6	A Bimetallic Ag/Tiâ€Based Coordination Polymer as a Catalyst for Electrocatalytic CO <sub>2</sub> Reduction and Selective Sulfide Oxidation. European Journal of Inorganic Chemistry, 2022, 2022, .	2.0	2
7	Long-term stress and trait anxiety affect brain network balance in dynamic cognitive computations. Cerebral Cortex, 2022, 32, 2957-2971.	2.9	8
8	Metal-Directed Self-Assembly of {Ti <sub>8</sub> L <sub>2</sub> } Cluster-Based Coordination Polymers with Enhanced Photocatalytic Alcohol Oxidation Activity. Inorganic Chemistry, 2022, 61, 923-930.	4.0	6
9	Momentary click nitrile synthesis enabled by an aminoazanium reagent. Organic Chemistry Frontiers, 2022, 9, 3420-3427.	4.5	5
10	An ultrastable Ti-based metallocalixarene nanocage cluster with photocatalytic amine oxidation activity. Chemical Communications, 2022, 58, 6028-6031.	4.1	12
11	Heterometallic Polyoxotitanium Clusters as Bifunctional Electrocatalysts for Overall Water Splitting. Inorganic Chemistry, 2022, 61, 10151-10158.	4.0	5
12	Side-Chain Length and Dispersity in ROMP Polymers with Pore-Generating Side Chains for Gas Separations. Jacs Au, 2022, 2, 1610-1615.	7.9	9
13	Recent advances in the synthesis and transformation of <i>gem</i> -borylsilylalkanes. New Journal of Chemistry, 2021, 45, 14847-14854.	2.8	13
14	Accurate assembly of ferrocene-functionalized {Ti22Fc4} clusters with photocatalytic amine oxidation activity. Chemical Communications, 2021, 57, 2792-2795.	4.1	19
15	Nano- and Microspheres Containing Inorganic and Biological Nanoparticles: Self-Assembly and Electron Tomographic Analysis. Journal of the American Chemical Society, 2021, 143, 2822-2828.	13.7	3
16	Endoscopyâ€Assisted Transoral Approach to Resect Parapharyngeal Space Tumors: A Systematic Review and Metaâ€Analysis. Laryngoscope, 2021, 131, 2246-2253.	2.0	3
17	A Weighted-Time-Lag Method to Detect Lag Vegetation Response to Climate Variation: A Case Study in Loess Plateau, China, 1982–2013. Remote Sensing, 2021, 13, 923.	4.0	11
18	Comprehensive Analysis of Myeloid Signature Genes in Head and Neck Squamous Cell Carcinoma to Predict the Prognosis and Immune Infiltration. Frontiers in Immunology, 2021, 12, 659184.	4.8	13

#	Article	IF	CITATIONS
19	Neutral Cyclometalated Ir(III) Complexes with Pyridylpyrrole Ligand for Photocatalytic Hydrogen Generation from Water. Inorganic Chemistry, 2021, 60, 6266-6275.	4.0	15
20	S-Shaped Double Helicene Diimides: Synthesis, Self-Assembly, and Mechanofluorochromism. Organic Letters, 2021, 23, 6183-6188.	4.6	16
21	3D Uranyl Organic Frameworks Supported by Rigid Octadentate Carboxylate Ligand: Synthesis, Structure Diversity, and Luminescence Properties. Chemistry - A European Journal, 2021, 27, 10313-10322.	3.3	6
22	Rapid Access to <i>N</i> -Protected Sulfonimidoyl Fluorides: Divergent Synthesis of Sulfonamides and Sulfonimidamides. Organic Letters, 2021, 23, 3975-3980.	4.6	23
23	Experimental analysis of dual-rotor-support-casing system with blade-casing rubbing. Engineering Failure Analysis, 2021, 123, 105306.	4.0	13
24	Photoinduced Transition-Metal-Free Alkynylation of Alkyl Pinacol Boronates. CCS Chemistry, 2021, 3, 1718-1728.	7.8	28
25	Inelastic contact behaviors of nanosized single-asperity and multi-asperity on α-Fe surface: Molecular dynamic simulations. International Journal of Mechanical Sciences, 2021, 204, 106569.	6.7	12
26	Automated Largeâ€5cale Extraction of Whistlers Using Maskâ€5coring Regional Convolutional Neural Network. Geophysical Research Letters, 2021, 48, e2021GL093819.	4.0	5
27	The future directions of synthetic chemistry. Pure and Applied Chemistry, 2021, 93, 1463-1472.	1.9	0
28	A hybrid model of LSTM neural networks with a thermodynamic model for condition-based maintenance of compressor fouling. Measurement Science and Technology, 2021, 32, 124007.	2.6	7
29	Brain preparedness: The proactive role of the cortisol awakening response in hippocampal-prefrontal functional interactions. Progress in Neurobiology, 2021, 205, 102127.	5.7	11
30	Metal–Ligand Cooperation in Cp*Ir-Pyridylpyrrole Complexes: Rational Design and Catalytic Activity in Formic Acid Dehydrogenation and CO <sub>2</sub> Hydrogenation under Ambient Conditions. Inorganic Chemistry, 2021, 60, 16584-16592.	4.0	15
31	Efficient Electrochemical Water Oxidation Mediated by Pyridylpyrrole-Carboxylate Ruthenium Complexes. Inorganic Chemistry, 2021, 60, 15627-15634.	4.0	3
32	Synthesis of Allylboronates via Zweifelâ€ŧype Deprotonative Olefination. Advanced Synthesis and Catalysis, 2021, 363, 2403-2407.	4.3	5
33	Cd-Doped Polyoxotitanium Nanoclusters with a Modifiable Organic Shell for Photoelectrochemical Water Splitting. Inorganic Chemistry, 2021, 60, 19263-19269.	4.0	7
34	A novel splice variant of LOXL2 promotes progression of human papillomavirus–negative head and neck squamous cell carcinoma. Cancer, 2020, 126, 737-748.	4.1	16
35	Rational genomic optimization of DNA detection for human papillomavirus type 16 in head and neck squamous cell carcinoma. Head and Neck, 2020, 42, 688-697.	2.0	2
36	Aminoazanium of DABCO: An Amination Reagent for Alkyl and Aryl Pinacol Boronates. Angewandte Chemie - International Edition, 2020, 59, 2745-2749.	13.8	53

#	Article	IF	CITATIONS
37	Hetero diacylation of 1,1-diborylalkanes: Practical synthesis of 1,3-diketones. Chinese Chemical Letters, 2020, 31, 1911-1913.	9.0	9
38	Aminoazanium of DABCO: An Amination Reagent for Alkyl and Aryl Pinacol Boronates. Angewandte Chemie, 2020, 132, 2767-2771.	2.0	14
39	Monocarboxylate-driven structural growth in Calix[ <i>n</i> ]arene-polyoxotitanate hybrid systems: utility in hydrogen production from water. Chemical Communications, 2020, 56, 14035-14038.	4.1	21
40	Preparation and characterization of polybenzoxazine foam with flame retardancy. Polymers for Advanced Technologies, 2020, 31, 3095-3103.	3.2	7
41	Cobalt-Catalyzed Radical Hydrotrifluoroethylation of Styrenes with Trifluoroethyl Iodide. Organic Letters, 2020, 22, 6552-6556.	4.6	18
42	HPV E2, E4, E5 drive alternative carcinogenic pathways in HPV positive cancers. Oncogene, 2020, 39, 6327-6339.	5.9	48
43	Zinc complexes supported by pyridine- <i>N</i> -oxide ligands: synthesis, structures and catalytic Michael addition reactions. Dalton Transactions, 2020, 49, 12365-12371.	3.3	2
44	Arenesulfonyl Fluoride Synthesis via Copperâ€free Sandmeyerâ€type Fluorosulfonylation of Arenediazonium Salts. Chinese Journal of Chemistry, 2020, 38, 1107-1110.	4.9	33
45	Structural, spectroscopic and electronic properties of a family of face-shared bi-octahedral Ru <sub>2</sub> <sup>5+/6+</sup> complexes with a bridging 2,5-di(2-pyridyl)pyrrolide ligand. Dalton Transactions, 2020, 49, 7053-7059.	3.3	2
46	Accurate Regulating of Visible-Light Absorption in Polyoxotitanate–Calix[8]arene Systems by Ligand Modification. Inorganic Chemistry, 2020, 59, 7512-7519.	4.0	21
47	Optimal Pattern Synthesis of Linear Array and Broadband Design of Whip Antenna Using Grasshopper Optimization Algorithm. International Journal of Antennas and Propagation, 2020, 2020, 1-14.	1.2	15
48	Chemodivergent transformations of amides using gem-diborylalkanes as pro-nucleophiles. Nature Communications, 2020, 11, 3113.	12.8	44
49	Occurrence of polyoxouranium motifs in uranyl organic networks constructed by using silicon-centered carboxylate linkers: structures, spectroscopy and computation. Dalton Transactions, 2020, 49, 4155-4163.	3.3	10
50	UBE2O Promotes Progression and Epithelial–Mesenchymal Transition in Head and Neck Squamous Cell Carcinoma. OncoTargets and Therapy, 2020, Volume 13, 6191-6202.	2.0	6
51	Targeting Viral DNA and Promoter Hypermethylation in Salivary Rinses for Recurrent HPV-Positive Oropharyngeal Cancer. Otolaryngology - Head and Neck Surgery, 2020, 162, 512-519.	1.9	6
52	Cannabinoids Promote Progression of HPV-Positive Head and Neck Squamous Cell Carcinoma via p38 MAPK Activation. Clinical Cancer Research, 2020, 26, 2693-2703.	7.0	52
53	Cryptic Chemical Communication: Secondary Metabolic Responses Revealed by Microbial Coâ€culture. Chemistry - an Asian Journal, 2020, 15, 327-337.	3.3	27
54	miR-93-5p enhances migration and invasion by targeting RGMB in squamous cell carcinoma of the head and neck. Journal of Cancer, 2020, 11, 3871-3881.	2.5	25

#	Article	IF	CITATIONS
55	miRâ€30eâ€5p represses angiogenesis and metastasis by directly targeting AEGâ€1 in squamous cell carcinoma of the head and neck. Cancer Science, 2020, 111, 356-368.	3.9	45
56	Aberrant expression of CPSF1 promotes head and neck squamous cell carcinoma via regulating alternative splicing. PLoS ONE, 2020, 15, e0233380.	2.5	13
57	Reciprocal activation of HEY1 and NOTCH4 under SOX2 control promotes EMT in head and neck squamous cell carcinoma. International Journal of Oncology, 2020, 58, 226-237.	3.3	7
58	Molecular Sensors for NMR-Based Detection. Chemical Reviews, 2019, 119, 195-230.	47.7	82
59	Casing vibration response prediction of dual-rotor-blade-casing system with blade-casing rubbing. Mechanical Systems and Signal Processing, 2019, 118, 61-77.	8.0	84
60	MEG actualized by high-valent metal carrier transport. Nano Energy, 2019, 65, 104047.	16.0	40
61	Stereoselective Synthesis of Trisubstituted Vinylboronates from Ketone Enolates Triggered by 1,3â€Metalate Rearrangement of Lithium Enolates. Angewandte Chemie, 2019, 131, 15960-15965.	2.0	10
62	Stereoselective Synthesis of Trisubstituted Vinylboronates from Ketone Enolates Triggered by 1,3â€Metalate Rearrangement of Lithium Enolates. Angewandte Chemie - International Edition, 2019, 58, 15813-15818.	13.8	38
63	α-C–H borylation of secondary alcohols <i>via</i> Ru/Fe relay catalysis: building a platform for alcoholic C–H/C–O functionalizations. Chemical Communications, 2019, 55, 11884-11887.	4.1	18
64	Cooperation between an alcoholic proton and boryl species in the catalytic <i>gem</i> -hydrodiborylation of carboxylic esters to access 1,1-diborylalkanes. Organic Chemistry Frontiers, 2019, 6, 900-907.	4.5	30
65	Intermolecular oxidative radical fluoroalkylfluorosulfonylation of unactivated alkenes with (fluoroalkyl)trimethylsilane, silver fluoride, sulfur dioxide and <i>N</i> -fluorobenzenesulfonimide. Organic Chemistry Frontiers, 2019, 6, 447-450.	4.5	46
66	Recent advances in the borylative transformation of carbonyl and carboxyl compounds. Organic and Biomolecular Chemistry, 2019, 17, 6099-6113.	2.8	37
67	Wnt3a promotes radioresistance via autophagy in squamous cell carcinoma of the head and neck. Journal of Cellular and Molecular Medicine, 2019, 23, 4711-4722.	3.6	38
68	Chromatin dysregulation and DNA methylation at transcription start sites associated with transcriptional repression in cancers. Nature Communications, 2019, 10, 2188.	12.8	61
69	Chaotic Adaptive Butterfly Mating Optimization and Its Applications in Synthesis and Structure Optimization of Antenna Arrays. International Journal of Antennas and Propagation, 2019, 2019, 1-14.	1.2	10
70	Corrections to "Approximated Solutions for ELF Near-Field Propagation Due to a Horizontal Electric Dipole Excitation Near the Sea-Rock Boundary―[May 18 2471-2481]. IEEE Transactions on Antennas and Propagation, 2019, 67, 4319-4319.	5.1	0
71	Polymers with Side Chain Porosity for Ultrapermeable and Plasticization Resistant Materials for Gas Separations. Advanced Materials, 2019, 31, e1807871.	21.0	64
72	Mutation of chromatin regulators and focal hotspot alterations characterize human papillomavirus–positive oropharyngeal squamous cell carcinoma. Cancer, 2019, 125, 2423-2434.	4.1	22

#	Article	IF	CITATIONS
73	Deoxygenative Transformation of Carbonyl and Carboxyl Compounds Using gem-Diborylalkanes. Synlett, 2019, 30, 1105-1110.	1.8	6
74	A Novel HF Broadband Frequency-Reconfigurable Whip Antenna With Radiation Blades Loading. IEEE Access, 2019, 7, 168944-168955.	4.2	1
75	Wnt3a protein overexpression predicts worse overall survival in laryngeal squamous cell carcinoma. Journal of Cancer, 2019, 10, 4633-4638.	2.5	7
76	Vibration propagation identification of rotor-bearing-casing system using spatiotemporal graphical modeling. Mechanism and Machine Theory, 2019, 134, 24-38.	4.5	3
77	Zincâ€Mediated Intermolecular Reductive Radical Fluoroalkylsulfination of Unsaturated Carbon–Carbon Bonds with Fluoroalkyl Bromides and Sulfur Dioxide. Chemistry - A European Journal, 2019, 25, 1824-1828.	3.3	45
78	Fault diagnosis of wind turbine based on Long Short-term memory networks. Renewable Energy, 2019, 133, 422-432.	8.9	327
79	Oxidative Radical Intermolecular Trifluoromethylthioarylation of Styrenes by Arenediazonium Salts and Copper(I) Trifluoromethylthiolate. Journal of Organic Chemistry, 2018, 83, 5836-5843.	3.2	25
80	Copper(ii)-catalyzed trifluoromethylation of iodoarenes using Chen's reagent. Organic Chemistry Frontiers, 2018, 5, 1143-1147.	4.5	17
81	Multivariate exploration of non-intrusive load monitoring via spatiotemporal pattern network. Applied Energy, 2018, 211, 1106-1122.	10.1	61
82	Photoinduced hydroxylperfluoroalkylation of styrenes. Organic Chemistry Frontiers, 2018, 5, 1045-1048.	4.5	34
83	Dual Functionalization of αâ€Monoboryl Carbanions through Deoxygenative Enolization with Carboxylic Acids. Angewandte Chemie, 2018, 130, 5599-5603.	2.0	25
84	An unsupervised spatiotemporal graphical modeling approach for wind turbine condition monitoring. Renewable Energy, 2018, 127, 230-241.	8.9	58
85	Iron(III) Porphyrin Catalyzed Olefination of Aldehydes with 2,2,2â€Trifluorodiazoethane (CF <sub>3</sub> CHN <sub>2</sub> ). European Journal of Organic Chemistry, 2018, 2018, 2082-2090.	2.4	17
86	Dual Functionalization of αâ€Monoboryl Carbanions through Deoxygenative Enolization with Carboxylic Acids. Angewandte Chemie - International Edition, 2018, 57, 5501-5505.	13.8	67
87	The <i>NOTCH4</i> – <i>HEY1</i> Pathway Induces Epithelial–Mesenchymal Transition in Head and Neck Squamous Cell Carcinoma. Clinical Cancer Research, 2018, 24, 619-633.	7.0	63
88	Synthesis of Secondary and Tertiary Alkyl Boronic Esters by <i>gem</i> â€Carboborylation: Carbonyl Compounds as Bis(electrophile) Equivalents. Angewandte Chemie, 2018, 130, 10475-10479.	2.0	15
89	KDM5B overexpression predicts a poor prognosis in patients with squamous cell carcinoma of the head and neck. Journal of Cancer, 2018, 9, 198-204.	2.5	24
90	Tumor-associated macrophages derived CCL18 promotes metastasis in squamous cell carcinoma of the head and neck. Cancer Cell International, 2018, 18, 120.	4.1	42

#	Article	IF	CITATIONS
91	Corrections to "A Novel Elliptical-Cylindrical Antenna Array for Radar Applications―[May 16 1681-1688]. IEEE Transactions on Antennas and Propagation, 2018, 66, 4386-4386.	5.1	0
92	Characterization of Alternative Splicing Events in HPV-Negative Head and Neck Squamous Cell Carcinoma Identifies an Oncogenic DOCK5 Variant. Clinical Cancer Research, 2018, 24, 5123-5132.	7.0	36
93	Discovery and development of differentially methylated regions in human papillomavirusâ€related oropharyngeal squamous cell carcinoma. International Journal of Cancer, 2018, 143, 2425-2436.	5.1	35
94	A Glycal Approach to the Synthesis of Pregnane Glycoside P57. Chinese Journal of Chemistry, 2018, 36, 1007-1010.	4.9	8
95	Synthesis of Secondary and Tertiary Alkyl Boronic Esters by <i>gem</i> â€Carboborylation: Carbonyl Compounds as Bis(electrophile) Equivalents. Angewandte Chemie - International Edition, 2018, 57, 10318-10322.	13.8	44
96	COMBINED ELECTROMECHANICAL ANALYSIS FOR A VERY-LOW-FREQUENCY COMPLEX STRUCTURE T-TYPE TRANSMITTING ANTENNA. Progress in Electromagnetics Research M, 2018, 63, 107-117.	0.9	0
97	Guided-mode-resonance coupled localized surface plasmons for dually resonance enhanced Raman scattering sensing. Proceedings of SPIE, 2017, , .	0.8	0
98	miR-185-3p regulates the invasion and metastasis of nasopharyngeal carcinoma by targeting WNT2B in vitro. Oncology Letters, 2017, 13, 2631-2636.	1.8	44
99	Autophagy inhibition impairs the epithelial-mesenchymal transition and enhances cisplatin sensitivity in nasopharyngeal carcinoma. Oncology Letters, 2017, 13, 4147-4154.	1.8	29
100	Influence Analysis of Nonlinear Stress–Strain Behavior in Pulverizing Wheel of Fan Mill. Journal of Failure Analysis and Prevention, 2017, 17, 571-580.	0.9	0
101	Models and Raman analysis of molecular nanofilms conjugated on photonic crystal slabs. , 2017, , .		0
102	C–O Functionalization of α-Oxyboronates: A Deoxygenative <i>gem</i> -Diborylation and <i>gem</i> -Silylborylation of Aldehydes and Ketones. Journal of the American Chemical Society, 2017, 139, 5257-5264.	13.7	142
103	Oxidative decarboxylative radical trifluoromethylthiolation of alkyl carboxylic acids with silver( <scp>i</scp> ) trifluoromethanethiolate and selectfluor. RSC Advances, 2017, 7, 880-883.	3.6	15
104	Trifluoromethylfluorosulfonylation of Unactivated Alkenes Using Readily Available Ag(O <sub>2</sub> CCF <sub>2</sub> SO <sub>2</sub> F) and <i>N</i> &€Fluorobenzenesulfonimide. Angewandte Chemie - International Edition, 2017, 56, 15432-15435.	13.8	63
105	Trifluoromethylfluorosulfonylation of Unactivated Alkenes Using Readily Available Ag(O <sub>2</sub> CCF <sub>2</sub> SO <sub>2</sub> F) and <i>N</i> â€Fluorobenzenesulfonimide. Angewandte Chemie, 2017, 129, 15634-15637.	2.0	19
106	An unsupervised anomaly detection approach using energy-based spatiotemporal graphical modeling. Cyber-Physical Systems, 2017, 3, 66-102.	2.0	25
107	miR-324-3p suppresses migration and invasion by targeting WNT2B in nasopharyngeal carcinoma. Cancer Cell International, 2017, 17, 2.	4.1	66
108	Non-Foster Matching Circuit Design via Tunable Inductor for VLF Receive Loop Antennas. International Journal of Antennas and Propagation, 2017, 2017, 1-10.	1.2	5

#	Article	IF	CITATIONS
109	An improved adaptive-step butterfly mating optimization algorithm. , 2017, , .		1
110	A novel DRM broadcast transmitting system based on circular array in medium wave. , 2017, , .		0
111	A MOMENT-BASED STUDY ON THE IMPEDANCE EFFECT OF MUTUAL COUPLING FOR VLF UMBRELLA ANTENNA ARRAYS. Progress in Electromagnetics Research C, 2017, 76, 75-86.	0.9	4
112	RSF1 regulates the proliferation and paclitaxel resistance via modulating NF-κB signaling pathway in nasopharyngeal carcinoma. Journal of Cancer, 2017, 8, 354-362.	2.5	19
113	A NOVEL BINARY BUTTERFLY MATING OPTIMIZATION ALGORITHM WITH SUBARRAY STRATEGY FOR THINNING OF LARGE ANTENNA ARRAY. Progress in Electromagnetics Research M, 2017, 60, 101-110.	0.9	7
114	Relational Utility Affects Self-Punishment in Direct and Indirect Reciprocity Situations. Social Psychology, 2017, 48, 19-27.	0.7	12
115	Using tDCS to Explore the Role of the Right Temporo-Parietal Junction in Theory of Mind and Cognitive Empathy. Frontiers in Psychology, 2016, 7, 380.	2.1	72
116	Memory consolidation reconfigures neural pathways involved in the suppression of emotional memories. Nature Communications, 2016, 7, 13375.	12.8	53
117	Genome-wide analyses of long noncoding RNA expression profiles correlated with radioresistance in nasopharyngeal carcinoma via next-generation deep sequencing. BMC Cancer, 2016, 16, 719.	2.6	54
118	Trifluoromethylation of haloarenes with a new trifluoro-methylating reagent Cu(O <sub>2</sub> CCF <sub>2</sub> SO <sub>2</sub> F) <sub>2</sub> . RSC Advances, 2016, 6, 50250-50254.	3.6	24
119	Comprehensive structural analysis and optimization of the electrostatic forming membrane reflector deployable antenna. Aerospace Science and Technology, 2016, 53, 267-279.	4.8	33
120	Next generation deep sequencing identified a novel lncRNA n375709 associated with paclitaxel resistance in nasopharyngeal carcinoma. Oncology Reports, 2016, 36, 1861-1867.	2.6	44
121	Palladium-catalyzed Sonogashira coupling of amides: access to ynones via C–N bond cleavage. Chemical Communications, 2016, 52, 12076-12079.	4.1	90
122	Supramolecular Differentiation for Construction of Anisotropic Fullerene Nanostructures by Time-Programmed Control of Interfacial Growth. ACS Nano, 2016, 10, 8796-8802.	14.6	82
123	Non-Foster matching network design for VLF receive loop antenna. IEICE Electronics Express, 2016, 13, 20160460-20160460.	0.8	6
124	Screening of Small-Molecule Inhibitors of Protein–Protein Interaction with Capillary Electrophoresis Frontal Analysis. Analytical Chemistry, 2016, 88, 8050-8057.	6.5	25
125	lonizing radiation promotes advanced malignant traits in nasopharyngeal carcinoma via activation of epithelial-mesenchymal transition and the cancer stem cell phenotype. Oncology Reports, 2016, 36, 72-78.	2.6	23
126	Diffusion of responsibility attenuates altruistic punishment: A functional magnetic resonance imaging effective connectivity study. Human Brain Mapping, 2016, 37, 663-677.	3.6	59

Chao Liu

#	Article	IF	CITATIONS
127	<scp>d</scp> -Alanylation in the Assembly of Ansatrienin Side Chain Is Catalyzed by a Modular NRPS. ACS Chemical Biology, 2016, 11, 876-881.	3.4	16
128	Rational Synthesis of Three-Dimensional Nanosuperstructures for Applications in Energy Storage and Conversion. IEEE Transactions on Device and Materials Reliability, 2016, 16, 475-482.	2.0	2
129	Interpersonal brain synchronization in the right temporo-parietal junction during face-to-face economic exchange. Social Cognitive and Affective Neuroscience, 2016, 11, 23-32.	3.0	148
130	Neural evidence for moral intuition and the temporal dynamics of interactions between emotional processes and moral cognition. Social Neuroscience, 2016, 11, 380-394.	1.3	32
131	A connectivity-based test-retest dataset of multi-modal magnetic resonance imaging in young healthy adults. Scientific Data, 2015, 2, 150056.	5.3	51
132	Language modulates brain activity underlying representation of kinship terms. Scientific Reports, 2015, 5, 18473.	3.3	4
133	In Vitro Reconstitution of a PKS Pathway for the Biosynthesis of Galbonolides in <i>Streptomyces</i> sp. LZ35. ChemBioChem, 2015, 16, 998-1007.	2.6	13
134	A cultural look at moral purity: wiping the face clean. Frontiers in Psychology, 2015, 6, 577.	2.1	22
135	Thinning of Concentric Circular Antenna Arrays Using Improved Binary Invasive Weed Optimization Algorithm. Mathematical Problems in Engineering, 2015, 2015, 1-8.	1.1	7
136	Chemical Pathways Connecting Lead(II) Iodide and Perovskite via Polymeric Plumbate(II) Fiber. Journal of the American Chemical Society, 2015, 137, 15907-15914.	13.7	223
137	Analysis of clinical features and prognosis of malignant triton tumor: A report of two cases and literature review. Oncology Letters, 2015, 10, 3551-3556.	1.8	28
138	Increased expression of miR-93 is associated with poor prognosis in head and neck squamous cell carcinoma. Tumor Biology, 2015, 36, 3949-3956.	1.8	38
139	Air-Stable and Solution-Processable Perovskite Photodetectors for Solar-Blind UV and Visible Light. Journal of Physical Chemistry Letters, 2015, 6, 535-539.	4.6	265
140	Influence of alternating loads on nonlinear vibration characteristics of cracked blade in rotor system. Journal of Sound and Vibration, 2015, 353, 205-219.	3.9	28
141	Fabrication and Robotization of Ultrasensitive Plasmonic Nanosensors for Molecule Detection with Raman Scattering. Sensors, 2015, 15, 10422-10451.	3.8	13
142	Review of recent advances in CF bond activation of aliphatic fluorides. Journal of Fluorine Chemistry, 2015, 179, 14-22.	1.7	208
143	Chinese Characteristic Religiosity: Comment on Jing (2014). Psychological Reports, 2015, 116, 322-323.	1.7	0
144	Heterologous expression of galbonolide biosynthetic genes in Streptomyces coelicolor. Antonie Van Leeuwenhoek, 2015, 107, 1359-1366.	1.7	13

#	Article	IF	CITATIONS
145	2,2,2-Trifluoroethylation of Styrenes with Concomitant Introduction of a Hydroxyl Group from Molecular Oxygen by Photoredox Catalysis Activated by Visible Light. Organic Letters, 2015, 17, 4714-4717.	4.6	81
146	Hierarchical pore-in-pore and wire-in-wire catalysts for rechargeable Zn– and Li–air batteries with ultra-long cycle life and high cell efficiency. Energy and Environmental Science, 2015, 8, 3274-3282.	30.8	107
147	Cortisol awakening response predicts intrinsic functional connectivity of the medial prefrontal cortex in the afternoon of the same day. NeuroImage, 2015, 122, 158-165.	4.2	18
148	Optimization design combined with coupled structural–electrostatic analysis for the electrostatically controlled deployable membrane reflector. Acta Astronautica, 2015, 106, 90-100.	3.2	13
149	Temporal Dynamics of the Integration of Intention and Outcome in Harmful and Helpful Moral Judgment. Frontiers in Psychology, 2015, 6, 2022.	2.1	18
150	Universal Enhancement of Raman Scattering Sensing by Plasmonic Nanotubes Coupled with Photonic Crystal Slab. , 2015, , .		0
151	The default mode network and social understanding of others: what do brain connectivity studies tell us. Frontiers in Human Neuroscience, 2014, 8, 74.	2.0	348
152	SYNTHESIS OF THINNED ARRAY WITH SIDE LOBE LEVELS REDUCTION USING IMPROVED BINARY INVASIVE WEED OPTIMIZATION. Progress in Electromagnetics Research M, 2014, 37, 21-30.	0.9	11
153	Pattern Synthesis of Planar Nonuniform Circular Antenna Arrays Using a Chaotic Adaptive Invasive Weed Optimization Algorithm. Mathematical Problems in Engineering, 2014, 2014, 1-13.	1.1	7
154	The Method for Broadband Folded Dipoles Using Branch Current Redistribution. Applied Mechanics and Materials, 2014, 548-549, 1381-1384.	0.2	0
155	Electric-Field Enhanced Molecule Detection in Suspension on Assembled Plasmonic Arrays by Raman Spectroscopy. Journal of Nanotechnology in Engineering and Medicine, 2014, 5, 0410051-410056.	0.8	1
156	The Research of Pattern Synthesis of Linear Antenna Array Based on Seeker Optimization Algorithm. , 2014, , .		1
157	β-Perfluoroalkylated meso-Aryl-Substituted Subporphyrins: Synthesis and Properties. Synthesis, 2014, 46, 1674-1688.	2.3	7
158	Location deterministic biosensing from quantum-dot-nanowire assemblies. Applied Physics Letters, 2014, 105, 083123.	3.3	8
159	miRâ€185â€3p regulates nasopharyngeal carcinoma radioresistance by targeting <scp>WNT</scp> 2B <i>in vitro</i> . Cancer Science, 2014, 105, 1560-1568.	3.9	63
160	Electricâ€Driven Rotation of Silicon Nanowires and Silicon Nanowire Motors. Advanced Functional Materials, 2014, 24, 4843-4850.	14.9	28
161	Crack modeling of rotating blades with cracked hexahedral finite element method. Mechanical Systems and Signal Processing, 2014, 46, 406-423.	8.0	40
162	Degradation of methiocarb by monochloramine in water treatment: Kinetics and pathways. Water Research, 2014, 50, 237-244.	11.3	12

#	Article	IF	CITATIONS
163	Calculation on characteristics of VLF umbrella inverted-cone transmitting antenna. , 2014, , .		3
164	Three-dimensional multilevel porous thin graphite nanosuperstructures for Ni(OH) <sub>2</sub> -based energy storage devices. Journal of Materials Chemistry A, 2014, 2, 15768-15773.	10.3	42
165	A General, Regiospecific Synthetic Route to Perfluoroalkylated Arenes via Arenediazonium Salts with R <sub>F</sub> Cu(CH <sub>3</sub> CN) Complexes. European Journal of Organic Chemistry, 2014, 2014, 6303-6309.	2.4	24
166	A Facile Way for Synthesis of High Performance Electron Receptor MCB: A Promising Replacer of PCBM. Fullerenes Nanotubes and Carbon Nanostructures, 2014, 22, 289-298.	2.1	4
167	Enhancement in the efficiency of an organic–inorganic hybrid solar cell with a doped P3HT hole-transporting layer on a void-free perovskite active layer. Journal of Materials Chemistry A, 2014, 2, 13827-13830.	10.3	163
168	Broadband Matching Network Design for Antennas Using Invasive Weed Optimization Algorithm. , 2013, , .		1
169	The representation of category typicality in the frontal cortex and its cross-linguistic variations. Brain and Language, 2013, 127, 415-427.	1.6	7
170	Photovoltaic performance optimization of methyl 4-[6,6]-C61-benzoate based polymer solar cells with thermal annealing approach. Synthetic Metals, 2013, 181, 117-122.	3.9	6
171	One-step waferscale synthesis of 3-D ZnO nanosuperstructures by designed catalysts for substantial improvement of solar water oxidation efficiency. Journal of Materials Chemistry A, 2013, 1, 8111.	10.3	18
172	Core Expansion of Perylenetetracarboxdiimide Dyes with Anthraquinone Units for Electronâ€Accepting Materials. European Journal of Organic Chemistry, 2013, 2013, 300-306.	2.4	13
173	Adaptive pattern nulling design of linear array antenna by phase perturbations using invasive weed optimization algorithm. , 2013, , .		1
174	Synthesis of Novel Acceptor Molecules of Mono- and Multiadduct Fullerene Derivatives for Improving Photovoltaic Performance. ACS Applied Materials & Interfaces, 2013, 5, 1061-1069.	8.0	22
175	Design and synthesis of β-multi-substituted push–pull porphyrins. RSC Advances, 2013, 3, 8227.	3.6	14
176	The Numerical Simulation of Electrical Characteristic for a New Material Antenna. Advanced Materials Research, 2013, 716, 586-589.	0.3	0
177	Electrode configuration optimization of the electrostatic forming membrane reflector. , 2013, , .		Ο
178	The male advantage in child facial resemblance detection: Behavioral and ERP evidence. Social Neuroscience, 2013, 8, 555-567.	1.3	25
179	Shape control of membrane reflector with electrostatic forming. , 2013, , .		0
180	Dissociable Somatotopic Representations of Chinese Action Verbs in the Motor and Premotor Cortex. Scientific Reports, 2013, 3, 2049.	3.3	20

#	Article	IF	CITATIONS
181	Genome-Wide Analyses of Radioresistance-Associated miRNA Expression Profile in Nasopharyngeal Carcinoma Using Next Generation Deep Sequencing. PLoS ONE, 2013, 8, e84486.	2.5	60
182	PLANAR ARRAY SYNTHESIS WITH SIDELOBE REDUCTION AND NULL CONTROL USING INVASIVE WEED OPTIMIZATION. Progress in Electromagnetics Research M, 2013, 33, 83-94.	0.9	3
183	A dual sensor of fluorescent and colorimetric for the rapid detection of lead. Analyst, The, 2012, 137, 1446.	3.5	16
184	Synthesis of (4-Hexyloxybenzoyl)butylsaure Methyl Amide/Poly(3-hexylthiophene) Heterojunction Nanowire Arrays. ACS Applied Materials & Interfaces, 2012, 4, 4841-4845.	8.0	6
185	Tuning Growth of Low-Dimensional Organic Nanostructures for Efficient Optical Waveguide Applications. Journal of Physical Chemistry C, 2012, 116, 14134-14138.	3.1	32
186	Suppression of aversive memories associates with changes in early and late stages of neurocognitive processing. Neuropsychologia, 2012, 50, 2839-2848.	1.6	39
187	The Time Course of the Influence of Valence and Arousal on the Implicit Processing of Affective Pictures. PLoS ONE, 2012, 7, e29668.	2.5	47
188	A NOVEL DUAL-POLARIZED ANTENNA WITH HIGH ISOLATION AND LOW CROSS POLARIZATION FOR WIRELESS COMMUNICATION. Progress in Electromagnetics Research Letters, 2012, 32, 129-136.	0.7	24
189	Synthesis and Photovoltaic Properties of Novel Monoadducts and Bisadducts Based on Amide Methanofullerene. ACS Applied Materials & Interfaces, 2012, 4, 1065-1071.	8.0	36
190	Compact Broadband Crescent Moon-Shape Patch-Pair Antenna. IEEE Antennas and Wireless Propagation Letters, 2011, 10, 435-437.	4.0	16
191	The processes leading to deception: ERP spatiotemporal principal component analysis and source analysis. Social Neuroscience, 2011, 6, 348-359.	1.3	14
192	Size-Dependent Surface Effects on the Photoluminescence in ZnO Nanorods. Journal of Physical Chemistry C, 2011, 115, 58-64.	3.1	63
193	Construction of a functional [2]rotaxane with multilevel fluorescence responses. Organic and Biomolecular Chemistry, 2011, 9, 7500.	2.8	16
194	Controllable growth and optical properties of ZnO nanostructures on Si nanowire arrays. CrystEngComm, 2011, 13, 2439.	2.6	25
195	Self-catalysis induced three-dimensional SiOx nanostructures. CrystEngComm, 2011, 13, 5807.	2.6	3
196	Multi-Representation of Symbolic and Nonsymbolic Numerical Magnitude in Chinese Number Processing. PLoS ONE, 2011, 6, e19373.	2.5	11
197	Eyes Are Windows to the Chinese Soul: Evidence from the Detection of Real and Fake Smiles. PLoS ONE, 2011, 6, e19903.	2.5	23
198	Temperature-dependent photoluminescence properties of porous silicon nanowire arrays. Applied Physics Letters, 2011, 99, 123106.	3.3	27

#	Article	IF	CITATIONS
199	Identification of about 100-meV acceptor level inÂZnOÂnanostructures by photoluminescence. Applied Physics A: Materials Science and Processing, 2011, 104, 695-699.	2.3	1
200	Strong Chargeâ€Transfer Chromophores from [2+2] Cycloadditions of TCNE and TCNQ to Peripheral Donorâ€Substituted Alkynes. European Journal of Organic Chemistry, 2011, 2011, 6445-6451.	2.4	34
201	Nanometerâ€Sized Reactor—A Porphyrinâ€Based Model System for Anion Species. Chemistry - A European Journal, 2011, 17, 7499-7505.	3.3	16
202	Local super-saturation dependent synthesis of MgO nanosheets. Applied Surface Science, 2011, 257, 3607-3611.	6.1	17
203	Acceptor-related emissions in indium-doped ZnO nanorods. Journal of Applied Physics, 2011, 109, 053507.	2.5	12
204	Brain Activity Elicited by Positive and Negative Feedback in Preschool-Aged Children. PLoS ONE, 2011, 6, e18774.	2.5	24
205	Highly efficient orange emission in ZnO:Se nanorods. Journal of Applied Physics, 2010, 108, .	2.5	11
206	What's in a name? Brain activity reveals categorization processes differ across languages. Human Brain Mapping, 2010, 31, 1786-1801.	3.6	16
207	Correlation between the 3.31-eV emission and the doping level in indium-doped ZnO nanostructures. Solid State Communications, 2010, 150, 2303-2305.	1.9	5
208	Show your teeth or not: The role of the mouth and eyes in smiles and its cross-cultural variations. Behavioral and Brain Sciences, 2010, 33, 450-452.	0.7	7
209	Exploring the conceptual and semantic structure of human kinship: An experimental investigation of Chinese kin terms. Behavioral and Brain Sciences, 2010, 33, 392-394.	0.7	3
210	New Methanofullerenes Containing Amide as Electron Acceptor for Construction Photovoltaic Devices. Journal of Physical Chemistry C, 2009, 113, 21970-21975.	3.1	35
211	Photodegradation of etridiazole by UV radiation during drinking water treatment. Chemosphere, 2009, 76, 609-615.	8.2	21
212	A Closed-Form Solution for ELF Radiated Fields of a Line-Current Antenna in Earth-Ionosphere Waveguide. , 2009, , .		1
213	The draft genome of the transgenic tropical fruit tree papaya (Carica papaya Linnaeus). Nature, 2008, 452, 991-996.	27.8	964
214	The Visual Word Form Area: Evidence from an fMRI study of implicit processing of Chinese characters. NeuroImage, 2008, 40, 1350-1361.	4.2	101
215	Synthesis and Reactions of 20 ï€-Electron β-Tetrakis(trifluoromethyl)-meso-tetraphenylporphyrins. Journal of the American Chemical Society, 2007, 129, 5814-5815.	13.7	108
216	Practical and Efficient Synthesis of Variousmeso-Functionalized Porphyrins via Simple Ligand-Free Nickel-Catalyzed Câ^'O, Câ^'N, and Câ^'C Cross-Coupling Reactions. Journal of Organic Chemistry, 2007, 72, 2732-2736.	3.2	51

#	ARTICLE	IF	CITATIONS
217	NUMERIC CALCULATION OF INPUT IMPEDANCE FOR A GIANT VLF T-TYPE ANTENNA ARRAY. Progress in Electromagnetics Research, 2007, 75, 1-10.	4.4	8
218	Synthesis and Versatile Reactions of β-Azidotetraarylporphyrins. European Journal of Organic Chemistry, 2007, 2007, 1419-1422.	2.4	54
219	Synthesis and Versatile Reactions of β-Azidotetraarylporphyrins. European Journal of Organic Chemistry, 2007, 2007, 2888-2888.	2.4	4
220	Unexpected bromination ring-opening of tetraarylporphyrins. Chemical Communications, 2006, , 770.	4.1	21
221	Câ <sup>°</sup> 'F Bond Activation by Modified Sulfinatodehalogenation:Â Facile Synthesis and Properties of Novel Tetrafluorobenzoporphyrins by Direct Intramolecular Cyclization and Reductive Defluorinative Aromatization of Readily Available Î <sup>2</sup> -Perfluoroalkylated Porphyrins. Journal of Organic Chemistry, 2006, 71, 9772-9783.	3.2	22
222	Re-examine the Limitation of the Complex Poynting Theorem. , 2006, , .		0
223	Fluorous Biphasic Catalytic Oxidation of Alkenes and Aldehydes with Air and 2-Methylpropanal in the Presence of (β-Perfluoroalkylated tetraphenylporphyrin)cobalt Complexes. European Journal of Organic Chemistry, 2006, 2006, 2703-2706.	2.4	25
224	Chemistry of Difluorocarbene: Synthesis and Conversion of Difluoro(methylene)cyclopropanes. European Journal of Organic Chemistry, 2006, 2006, 5581-5587.	2.4	28
225	Unexpected Intramolecular Cyclization of 2-(Perfluoroalkyl)tetraarylporphyrin Radicals: Approaches for the Intramolecular Cyclization of 2-(Perfluoroalkyl)tetraarylporphyrin Radicals. European Journal of Organic Chemistry, 2005, 2005, 306-316.	2.4	22
226	Fluoroalkylation of Porphyrins: A Facile Synthesis of Trifluoromethylated Porphyrins by a Palladium-Catalyzed Cross-Coupling Reaction. European Journal of Organic Chemistry, 2005, 2005, 3680-3686.	2.4	49
227	Data Sources. , 2002, , 797-810.		0
228	Influence of Inhomogeneous Anisotropic Ground Conductivity upon the Directivity of ELF Line-Current Antenna. Applied Mechanics and Materials, 0, 548-549, 725-729.	0.2	0
229	The Impedance Characteristics of ELF Line-Current Antenna over Inhomogeneous Anisotropic Ground. Applied Mechanics and Materials, 0, 548-549, 771-775.	0.2	0
230	A novel integrated modeling approach for filter diagnosis in gas turbine air intake system. Proceedings of the Institution of Mechanical Engineers, Part A: Journal of Power and Energy, 0, , 095765092110443.	1.4	4